Mosaicking Airborne Scanner Data with the Multiquadric Rectification Technique

Kenneth C. McGwire

Abstract

A new multiquadric image rectification technique is shown to provide superior results for mosaicking nine flight lines of airborne scanner data covering 200 km² of hilly terrain with limited ground control. The multiquadric technique provided excellent edge matching and less than half the absolute geometric error of polynomial-based techniques.

Introduction

Traditional polynomial rectification techniques have generally proven inadequate for geometric correction of airborne scanner data, and several approaches have been pursued to deal with this difficulty (Devereaux *et al.*, 1990; Fischer, 1991; Chen and Rau, 1993; Fogel and Tinney, 1996). This paper presents the results of mosaicking aircraft scanner data from multiple flight lines using Hardy's multiquadric technique. The multiquadric method is an exact interpolator which is shown to provide superior results, both in the aesthetics of edge matching and in an independent test of geometric accuracy. Data were taken from a Deadelus NS001 scanner flown on a C-130 aircraft on 21 June 1994 over Fort Hunter Liggett in California with a nominal resolution of slightly less than four metres. Nine flight lines were mosaicked together to cover over 200 km² of hilly terrain with limited features for ground control. This work was part of a demonstration of the utility of airborne remote sensing for environmental analysis which was performed by Geo-Insight International of Ojai, California.

The NS001 scanner sweeps a 100° angle for each scan line. While this wide angle provides a reasonable swath width, the wide angular range also creates large geometric distortions in the raw image data. The data used in this study were pre-processed by personnel at the NASA Ames Research Center to correct this effect by interpolating off-nadir measurements to approximate a constant ground resolution. However, aircraft scanner imagery presents several additional challenges with respect to geometric fidelity, including instability of the aircraft platform during scanning and localized scale changes due to topography.

Most image processing software packages provide polynomial-based rectification methods in order to correct geometric distortions in image data. However, polynomial techniques are quite limited in their ability to handle the complex distortions found in aircraft scanner data. While higher order polynomials may fit more complex distortions, the results are often quite unstable and can easily provide worse results than simple first- or second-order fits (McGwire, 1996; Welch *et al.*, 1985). It was known that polynomial-based methods would be incapable of creating a seamless mosaic of airborne scanner data, especially given the hilly terrain and geometric distortions found in the study area. Two characteristics of the recently developed multiquadric, bi-harmonic method led to its selection for this purpose:

- it provides a global solution derived from all control points, thereby avoiding potential ambiguities in the triangulation of control points (Fogel, 1996) or discontinuities along fitted patches which may occur with local, piecewise methods (Jensen *et al.*, 1987); and
- it is an exact interpolator, allowing ground control points along mosaic seams to be perfectly matched.

The multiquadric technique is one of a family of methods referred to as radial basis functions. The reader is referred to Ehlers (1997), Fogel (1996), Goshtasby (1988), and Göpfert (1982) for detailed discussions of multiquadric rectification techniques. The following overview is summarized from Ehlers (1997). A simple polynomial transformation is first used to model the general geometric transformation. An interpolating function is then used to separately fit the vectors of residuals in **X** and **Y** at each control point. Weights (**A**) explaining the effect of local distortions measured at each control point (dX) are calculated using an interpolating matrix (**F**) developed from the Euclidean distance between control points (f_{ij}): i.e.,

$$\begin{bmatrix} dX_1 \\ dX_2 \\ \vdots \\ dX_n \end{bmatrix} = \begin{bmatrix} f_{11},\ldots & \ldots f_{1n} \\ f_{21},\ldots & \ldots f_{2n} \\ \vdots & \vdots \\ f_{n1},\ldots & \ldots f_{nn} \end{bmatrix} * \begin{bmatrix} a_1 \\ a_2 \\ \vdots \\ a_n \end{bmatrix}.$$

This results in n equations for n unknowns which are solved for **A**. **F** is symmetric and the system of equations has zeros at the diagonal. Solving for **A**, we obtain the residual improvements dX_k for $k = 1, 2, \ldots, n$: i.e.,

$$f_{k1}\, a_1 + f_{k2}\, a_2 + \ldots + f_{kn}\, a_n = dX_k.$$

This solution is then applied to each pixel in the image by using the Euclidean distance to each control point. The interpolating function may be adjusted by a user-specified smoothing factor.

The software used in this study was originally developed by Flottemesch (1993) with the name MQReg, then substantially refined and renamed to MQE by Fogel (Fogel and Tinney, 1996). It is currently planned that the MQE software will be made available through the National Center for Geographic Information and Analysis (NCGIA; www.ncgia.ucsb.edu).

Approach

Surface reflectance typically displays directional dependence which depends on the orientation of the light source, target, and scanner, as well as the wavelength, and may be characterized by a bi-directional reflectance distribution function (BRDF) (Deering and Middleton, 1990). BRDF effects in NS001

Desert Research Institute, Biological Sciences Center, 7010 Dandini Blvd., Reno, NV 89512 (kenm@dri.edu).

Photogrammetric Engineering & Remote Sensing, Vol. 64, No. 6, June 1998, pp. 601–606.

0099-1112/98/6406–601$3.00/0

imagery are apparent as a strong change in brightness as the sensor goes through its 100° scan angle (Figure 1a). For this demonstration, a first-order normalization was applied to reduce BRDF effects. Each vertical column of pixels from each original flightline was rescaled to a relatively constant brightness level prior to geometric correction by fitting a running mean to digital numbers (DNs) across the swath. This mean was generated from a wide band of lines in each image which contained a relatively constant mix of cover types and slope positions. Deviations of this running mean from the overall mean were then subtracted on a column-by-column basis. In order to avoid overall shifts in brightness between flight lines, the remaining difference in DNs between overlapping areas in each flightline were used to adjust each corrected flightline to a similar mean response. The results of this image normalization technique are demonstrated in Figure 1b. This method does not quantitatively deal with the fact that different land covers generally display a different BRDF. However, it is effective for minimizing abrupt discontinuities between flight lines in the mosaicked product.

The flight lines covering the study area provided approximately 60 percent sidelap between adjacent images, effectively duplicating all coverage of the study area. Thus, it would have been possible to reduce the processing burden by discarding every other flight line. However, this overlap provided a benefit which could be exploited to improve the geometric accuracy of the mosaicked product. By selecting only the central portion of each flight line and discarding overlap on the edges, topographic distortions were reduced by using only the "sweet-spot" which is closest to nadir. If a polynomial rectification were used, the potential reduction in topographic distortion might be offset by increased problems with edge matching when using more flight lines. In addition to reducing topographic distortions, limiting the angle of image acquisition further reduces the potential variability in spectral response between flight lines due to BRDF.

Image data were registered to control points digitized from USGS 7.5-minute quadrangles covering the study area. The number of available control points was limited, given both the remoteness of the location and the fact that the maps were quite out of date. In order to provide a seamless mosaic with the multiquadric technique, the rectification was performed in two stages. First, alternating flight lines were rectified to UTM ground control points (GCPs) from the USGS maps. Then, the "sweet-spot" was subset out of the center of intervening flight lines and these sub-images were rectified using

- the limited number of GCPs available from the USGS quadrangles, and
- a large number of control points derived from the first set of rectified images corresponding to features on the edges of each sub-image.

The first set from the quadrangles provided for quantitative image-to-map rectification, while the second set provided qualitative image-to-image registration along seams in the mosaic. This process is diagrammed for one set of flight lines in Figure 2. The high resolution of the NS001 imagery made the identification of image-to-image control points, or tie points, quite easy. The multiquadric rectification was performed using a first-order polynomial for the initial stage of

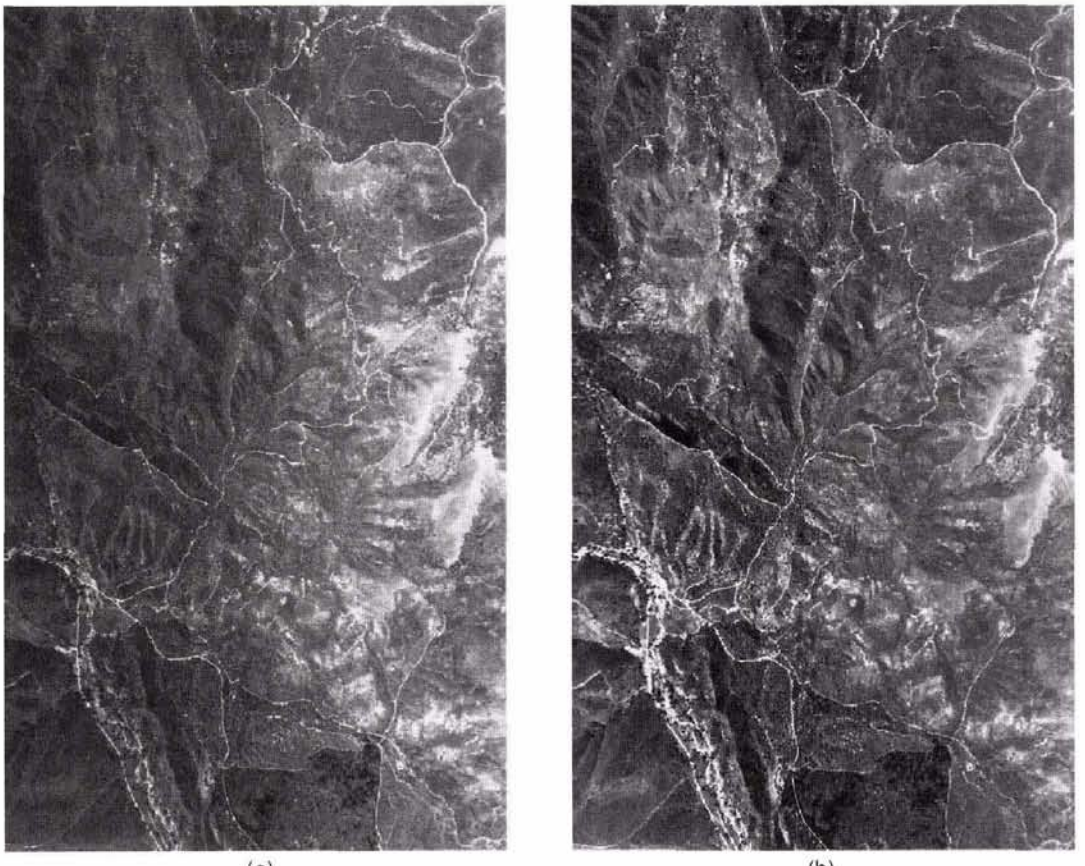

(a) (b)

Figure 1. Normalizing bidirectional reflectance: (a) segment of flight line prior to correction, (b) after correction.

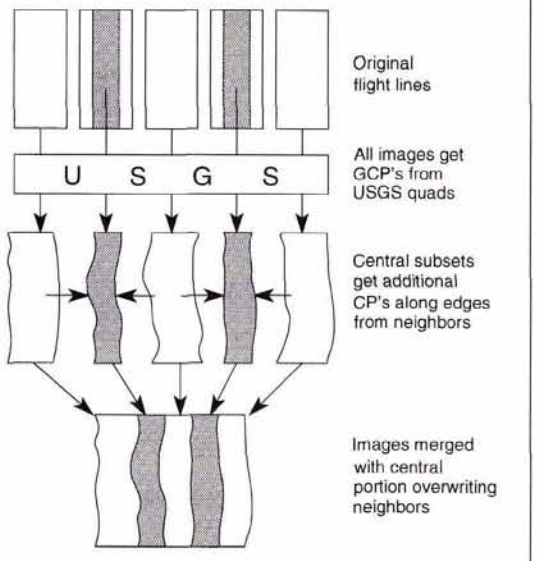

Figure 2. Overlaying intervening flight lines on corrected imagery.

correction. A default value for the multiquadric smoothing parameter, as approximated by Göpfert (1982), was provided by the software. Resampling was performed with a cubic convolution.

This method was then tested against the commonly used polynomial rectification method for a subset of the entire study area. The entire area of the multiquadric rectification is presented in Figure 3, with the area used for comparison with the polynomial method in an expanded view. Given the limitations of the polynomial method, it made no sense to attempt this comparison over the entire area. Any effort to do so would require a piecewise approach of the type performed by Jensen *et al.* (1987), resulting in additional visible discontinuities in the rectified product while substantially increasing the level of effort. The area to be compared covered a portion of five consecutive flight lines from the multiquadric rectification. The polynomial approach was tested using both five flight lines and three flight lines (making use of the 60 percent sidelap).

Polynomial rectifications were tested using a second-order fit. The simple affine transformation of a first-order polynomial was obviously insufficient. Higher order polynomials were not used because of their inherent instability and the limited availability of ground control. One attempt at a third-order correction yielded obviously inferior results. Corrected data were resampled to a four-metre resolution using cubic convolution for both the multiquadric and polynomial methods. Eleven independent check points were identified in the subarea to measure the geometric accuracy of the rectified products.

Results

The mosaicking of multiple flight lines into a seamless composite was achieved by

- taking advantage of the high degree of overlap between adjacent flight lines,
- mixing map and image based control points, and
- using the multiquadric image correction algorithm.

An example of the ability of the multiquadric technique to

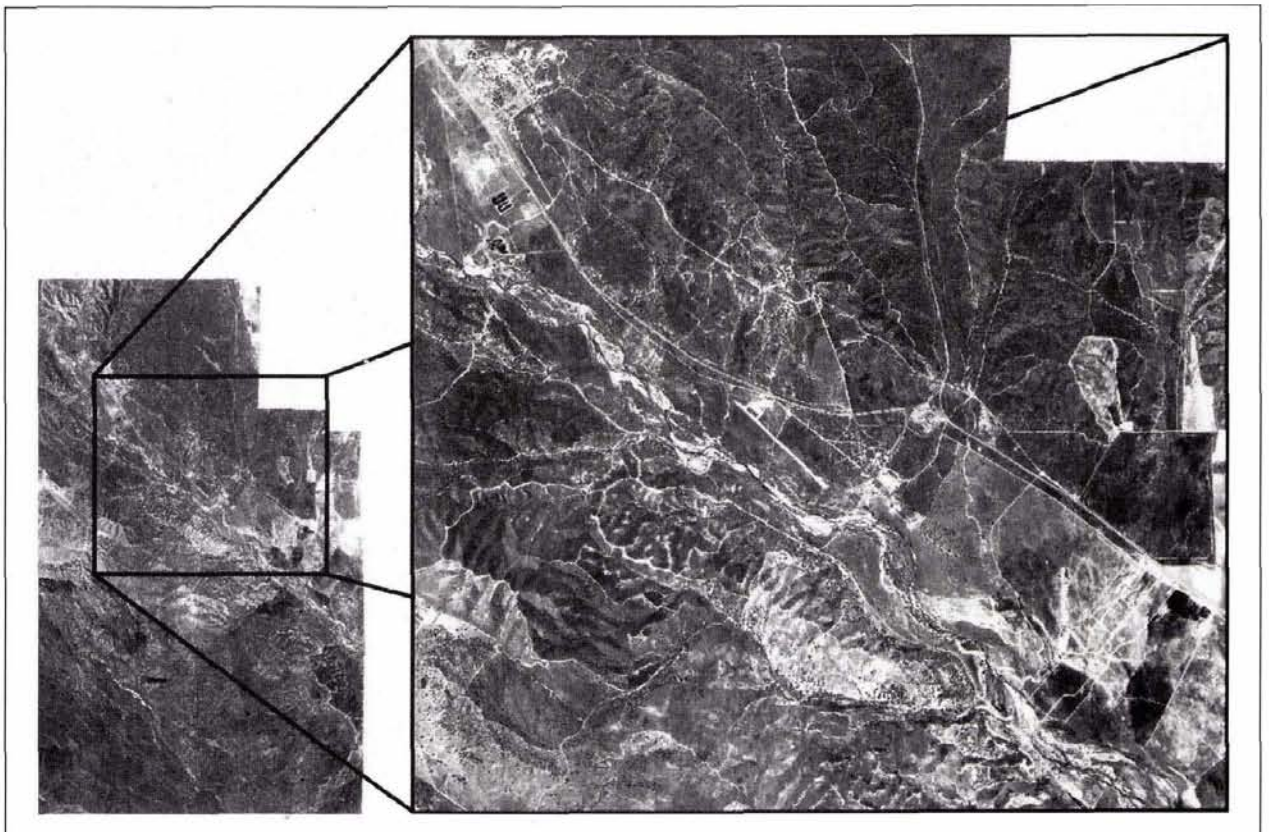

Figure 3. Subset from full mosaic selected for testing against ground control and polynomial techniques.

Figure 4. Example of the complex correction afforded by the multiquadric technique.

handle the geometric distortion in aircraft data is displayed in Figure 4. This figure displays a section of a flight line used in the Hunter Liggett mosaic. Notice that the edges demonstrate continuous and complex warping. The multiquadric method provided a virtually seamless composite across the entire study area displayed in Figure 3. Colleagues were unable to pick out many of the edges between adjacent flight lines, even though no filtering or feathering of edges had been applied whatsoever.

Figure 5 shows a zoomed in view of part of the multiquadric mosaic. Three seams run somewhere through this figure. The successful BRDF normalization and excellent registration make detection of these seams quite difficult. A certain amount of jitter is apparent in the resampling of DNs along linear features. This jitter was created by an error in the cubic convolution routine which was implemented at the time of this study. This problem has since been corrected.

Figure 6 shows an enlarged view of part of the mosaic created by the second-order polynomial with three flight lines. A single seam runs through the right side of this figure. The approximate location of this seam is indicated by tic mark on the bottom edge of the image. A sharp contrast in image tone is apparent, suggesting that the simplistic BRDF normalization was not capable of correcting brightness differences at extremely opposite look angles.

Figure 7 shows a zoomed in view of part of the mosaic created with the second-order polynomial and five flight lines. Three seams run through this figure, and their approximate locations are indicated by tic marks on the bottom edge of the image. Some of the offsets between flight lines are less noticeable than in Figure 6, due in part to a more consistent image tone. The three seams in Figure 7 indicate the general area where these seams exist in the multiquadric product portrayed in Figure 5.

Table 1. RMS Error of MQE vs. Polynomials (metres)

	Polynomial Three Flight Lines	Polynomial Five Flight Lines	Multiquadric Five Flight Lines
Transformation RMS	40 m	44 m	N/A
Check Point RMS	64 m	71 m	25 m

Table 1 presents the RMS error from transformation residuals and for the independent check points. Transformation residuals for the polynomial techniques underpredict actual error by 38 percent. This result is expected because the transformation residuals are not independent of the training data (McGwire, 1996; Ehlers, 1997). The polynomial method with three flight lines performed better than that with five flight lines. It is likely that this resulted from having fewer map-based control points available per image for the near-nadir subsets from intervening flight lines. The poor fit along seams of the five-flight-line mosaic actually led to a problem where one of the independent check points was visible in two places (the nearer one was selected for the RMSE statistic). This effect is most visible on the seam to the far left of Figure 7.

Because control points are matched exactly in the multiquadric technique, there are no transformation residuals to directly diagnose the expected geometric accuracy (Table 1). The cross-validation method described by McGwire (1996) could be used to generate an error estimate for such exact interpolators. However, this capability was not implemented at the time of the study. Also, such an approach would need to be tested with exact interpolators because their behavior is quite different than that of lower order polynomials. Geometric error in the multiquadric mosaic, as measured by independent test points, is less than half that of the better polynomial method and is quite good given the limited number of control points and the complex distortions involved. It is expected that, in the vicinity of the control points, this improvement is due predominantly to the ability of the multiquadric method to handle local distortions. At more distant locations, the reduction in topographic variability allowed by using near-nadir portions of flight lines likely increases in significance. This latter effect is facilitated by the multiquadric method because it allows near-perfect edge matching.

Conclusions

The multiquadric method provided excellent results in terms of appearance and absolute geometric accuracy and is well suited to the problems of airborne scanner data. The effectiveness of these results suggest that the traditional use of polynomial-based techniques be re-examined by the remote sensing community. New methods, such as the multiquadric technique and thin plate splines, have shown excellent results, and vendors are currently developing software for

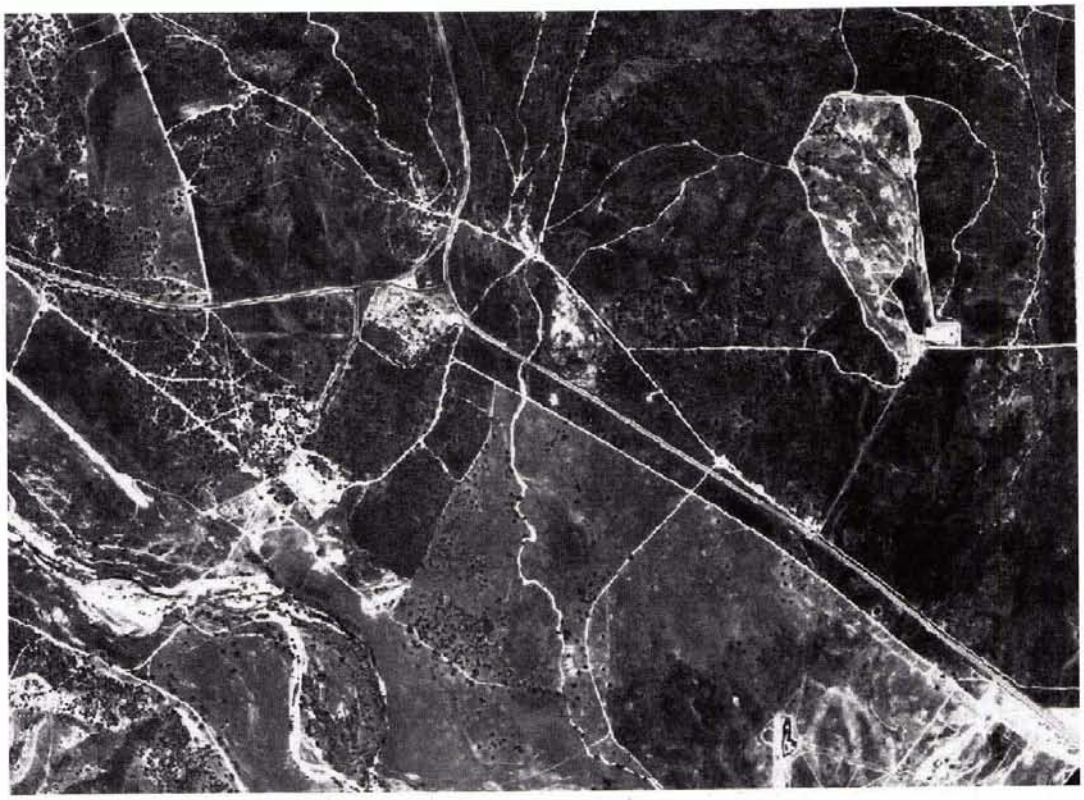

Figure 5. Detail from the mosaic using the multiquadric technique.

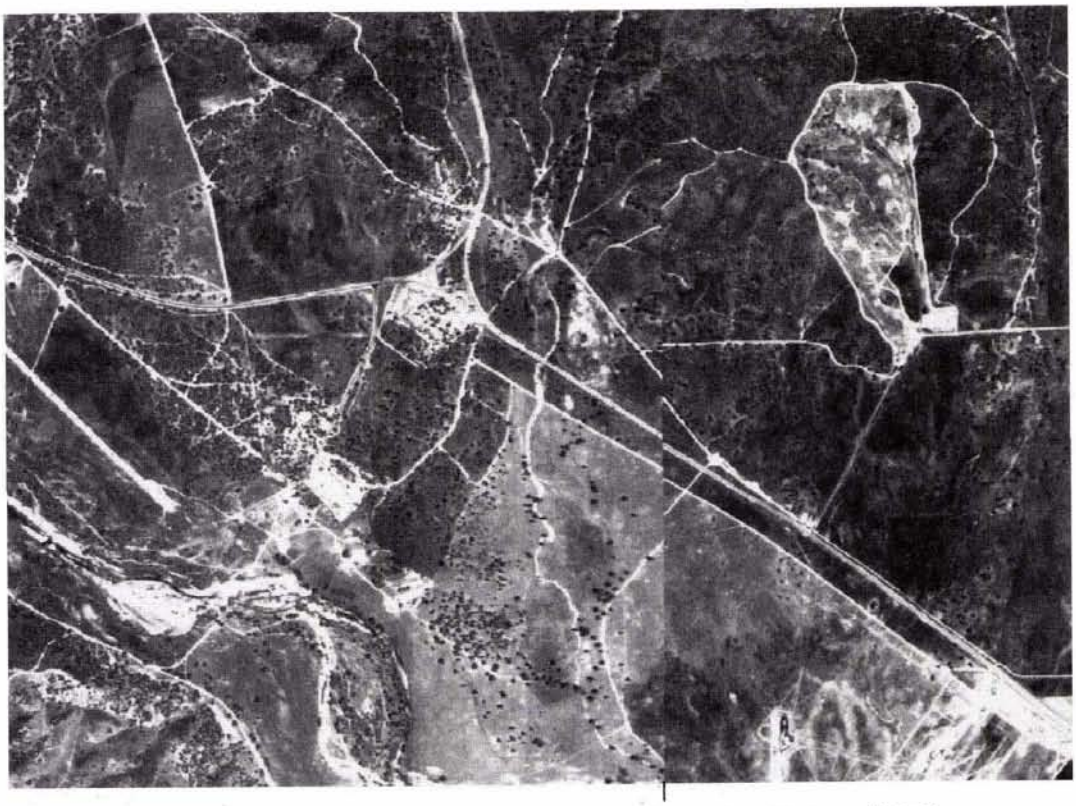

Figure 6. Detail for the test area for second-order polynomial with three flight lines.

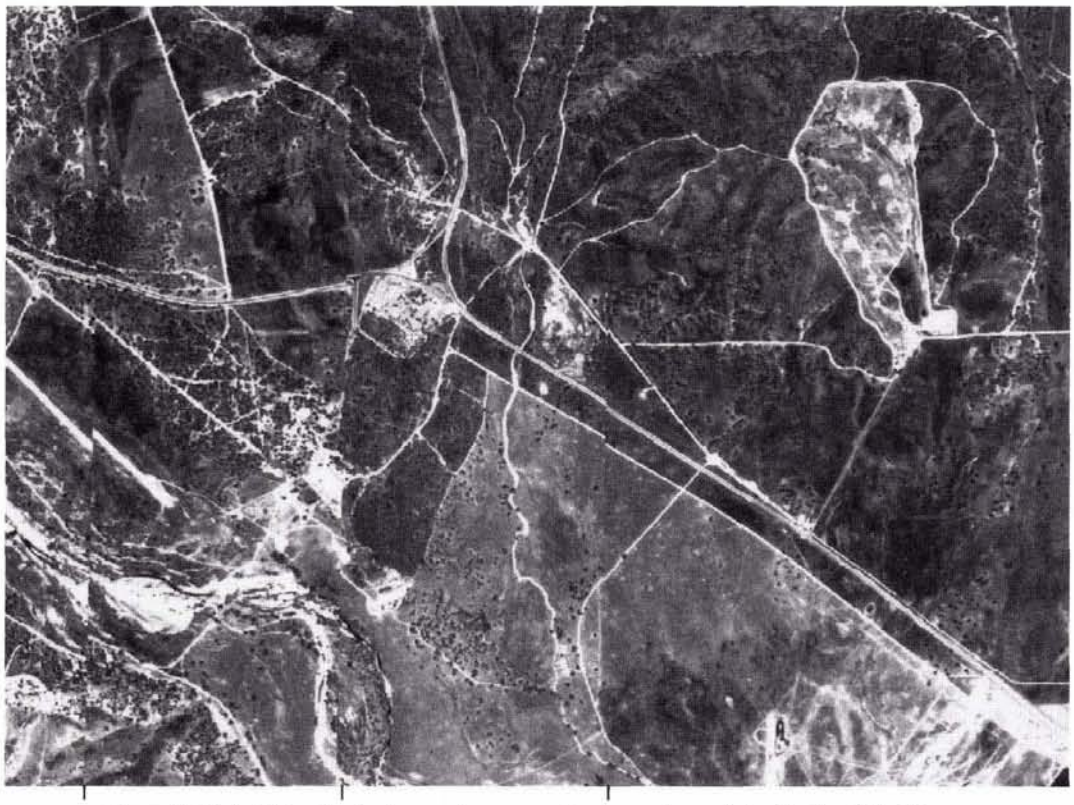

Figure 7. Detail for the test area for second-order polynomial with five flight lines.

these techniques. However, further research with the multiquadric method should include the effects of polynomial order used in the initial correction, the effects of the smoothing parameter, limitations on the numbers of control points which may be used, and possible biases in using cross-validated RMSE error statistics.

Acknowledgment

A special thanks to the excellent people of Geo-Insight International, an environmental consulting group in Ojai, California, who made this study possible by providing the data and the support for the Hunter-Liggett study. Special thanks to David Fogel who made an early version of the multiquadric code available. Thanks to Uwe Flottemesch and Manfred Ehlers for initial development of the multiquadric code. Further code development was supported in part by EG&G Energy Systems (PO 23787M), NASA (NAGW-1743), and the National Center for Geographic Information and Analysis (NSF SBR88-10917).

References

Deering, D., and E. Middleton, 1990. Spectral bidirectional reflectance and the effects on vegetation indices for a prairie grassland, *Proceedings, Symposium on FIFE*, American Meteorological Society, Boston.

Chen, L., and J. Rau, 1993. Geometric Correction of airborne scanner imagery using orthophotos and triangulated feature point matching, *International Journal of Remote Sensing*, 14(16):3041–3059.

Devereaux, B., R. Fuller, L. Carter, and R. Parsell, 1990. Geometric Correction of airborne scanner imagery by matching Delauney triangles, *International Journal of Remote Sensing*, 11(12):2237–2251.

Ehlers, M., 1997. Rectification and Registration, *Integration of Geographic Information Systems and Remote Sensing* (J. Star, J. Estes, and K. McGwire, editors), Cambridge University Press.

Fisher, L., 1991. Geometric correction of multispectral scanner data using global positioning system and digital terrain models, *Proceedings of a special session of the ACSM-ASPRS 1991 Annual Convention: The Integration of Remote Sensing and Geographic Information Systems* (J. Star, editor), American Society for Photogrammetry and Remote Sensing, Falls Church, Virginia.

Flottemesch, U., 1993. *Geometrische Entzerrung von digitalen Flugzeugscannerdaten mit der multiquadrischen Interpolation*. Diplomarbeit, Institut für Photogrammetrie und Ingernieurvermessungen, Universität Hannover (Master's Thesis).

Fogel, D., 1996. Image rectification with radial basis functions, *Proceedings, Third International Conference/Workshop on Integrating GIS and Environmental Modeling*, Santa Fe, New Mexico, 21–26 January 1996, CD-ROM, National Center for Geographic Information and Analysis, University of California, Santa Barbara.

Fogel, D., and L. Tinney, 1996. *Image Registration Using Multiquadric Functions*, Technical Report 96-01, National Center for Geographic Information and Analysis, University of California, Santa Barbara.

Göpfert, W., 1982. Methodology for Thematic Image Processing Using Thematic and Topographic Data Bases and Base-Integrated Multi-Sensor Imagery, *Proceedings, ISPRS Commission VII Symposium*, Toulouse, France, I:13–19.

Goshtasby, A., 1988. Registration of images with geometric distortion, *IEEE Transactions on Geoscience and Remote Sensing*, 26(1):60–64.

Jensen, J., E. Ramsey, H. Mackey, Jr., E. Christensen, and R. Sharitz, 1987. Inland wetland change detection using aircraft MSS data, *Photogrammetric Engineering & Remote Sensing*, 53(5):521–529.

McGwire, K., 1996. Cross-Validated Assesment of Geometric Accuracy, *Photogrammetric Engineering & Remote Sensing*, 62(10):1179–1187.

Welch, R., T. Jordan, and M. Ehlers, 1985. Comparative evaluations of the geodetic accuracy and cartographic potential of Landsat-4 and Landsat-5 Thematic Mapper image data, *Photogrammetric Engineering & Remote Sensing*, 51(9):1249–1262.

(Received 17 December 1996; accepted 17 November 1997; revised 5 December 1997)